Talanta 126 (2014) 208–213

Contents lists available at ScienceDirect

Talanta

journal homepage: www.elsevier.com/locate/talanta

Influence of carbon-based nanomaterials on *lux*-bioreporter *Escherichia coli*

Kun Jia [a], Robert S. Marks [b,c,d,e], Rodica E. Ionescu [a,*]

[a] Laboratoire de Nanotechnologie et d'Instrumentation Optique, Institute Charles Delaunay, Université de technologie de Troyes, UMR-CNRS 6281, 12 Rue Marie-Curie CS 42060, 10004 Troyes Cedex, France
[b] Department of Biotechnology Engineering, Faculty of Engineering Science, Ben-Gurion University of the Negev, PO Box 653, 84105 Beer-Sheva, Israel
[c] National Institute for Biotechnology in the Negev, Ben-Gurion University of the Negev, Beer-Sheva, Israel
[d] The Ilse Katz Centre for Meso and Nanoscale Science and Technology, Ben-Gurion University of the Negev, Beer-Sheva 84105, Israel
[e] School of Materials Science and Engineering, Nanyang Technological University, Singapore 637722, Singapore

ARTICLE INFO

Article history:
Received 16 December 2013
Received in revised form
10 March 2014
Accepted 13 March 2014
Available online 20 March 2014

Keywords:
Engineered *E. coli* bacteria
Bioluminescence
Carbon nanotube
Graphene nanosheet
Carbon black nanopowder

ABSTRACT

The cytotoxic effects of carbon-based nanomaterials are evaluated via the induction of luminescent genetically engineered *Escherichia coli* bacterial cells. Specifically, two engineered *E. coli* bacteria strains of DPD2794 and TV1061 were incubated with aqueous dispersion of three carbon allotropes (multi-wall carbon nanotubes (MWCNTs), graphene nanosheets and carbon black nanopowders) with different concentrations and the resulting bioluminescence was recorded at 30 °C and 25 °C, respectively. The corresponding optical density changes of bacterial cells in the presence of various carbon nanomaterials were recorded as well. Based on these results, *E. coli* DPD2794 bacterial induction responds to a greater degree than *E. coli* TV1061 bacteria when exposed to various carbon-based nanomaterials. Finally, the surface morphology of *E. coli* DPD2794 bacteria cells before and after carbon-based nanomaterials treatment was observed using a field emission scanning electron microscope (FESEM), from which morphological changes from the presence of carbon-based nanomaterials were observed and discussed.

1. Introduction

Owing to their excellent mechanical and tunable electronic properties, carbon-based nanomaterials (carbon nanotubes, graphene, fullerene, carbon black, etc.) have found wide applications in a range of fields such as biochemical sensors [1–3], alternative energy [4,5], nanomedicine [6,7] and high performance composite materials [8,9]. However, the environmental impact of carbon-based nanomaterials is crucial to understand before they are released in large scale into the environment. Issues such as dispersion, ecotoxicology and human health effects need to be systematically evaluated prior to their large-scale commercial use. Previously, it has been reported that cytotoxicity of carbon-based nanomaterials is dependent on their shape, size, surface modification and electronic structures [10]. For instance, single wall carbon nanotube (SWCNT) dispersions are highly cytotoxic to bacterial cells when dispersed uniformly in solution [11]. By using specialized microscopic (AFM or SEM) characterization, as well as gene expression methods, carbon nanotube cytotoxicity mechanisms to bacterial cells were evaluated as possibly involving a combination of direct cellular membrane stress and oxidative stress [12–14]. In addition, emerging 2D graphene nanosheet composites were shown to exhibit high toxicity to bacterial cells possibly due to the direct contact of their extremely sharp edge [15,16], thus hinting to their putative use as a novel antibacterial agent [17,18] or material, such as antibacterial paper, or film [19,20].

Over the years, bioluminescence of genetically modified bacterial cells has been explored in whole cell biosensor devices in the detection of various toxicants such as pesticides [21–23], heavy metals [24–27] and organic pollutants [28]. In this system, the plasmids of bacterial cells are genetically modified to include toxicant-specific promoter genes that regulate the expression of bioluminescence proteins [29]. For example, *Escherichia coli* strain TV1061 harbors a fusion of *luxCDABE* reporter gene and the promoter for the heat-shock gene *grpE*, while in the *E. coli* strain DPD2794, the promoter of *recA* gene is fused with *luxCDABE*. While TV1061 bacterial strain is responsive to many toxic compounds [30], the responses of DPD2794 bacterial cells are mainly restricted to that of genotoxicity [31]. When these bacterial cells are incubated with certain toxicants, bioluminescence is generated once the lux operon has been transcribed and translated to produce luciferase (encoded by *luxAB*) and its associated substrate (reduced flavin mononucleotide ($FMNH_2$) and long-chain fatty aldehyde, encoded by *luxCDE*), an event that is triggered by the adjacent promoter that is sensitive to certain given toxicants.

* Corresponding author. Tel.: +33 3 25 75 97 28; fax: +33 3 25 71 84 56.
E-mail address: elena_rodica.ionescu@utt.fr (R.E. Ionescu).

http://dx.doi.org/10.1016/j.talanta.2014.03.024
0039-9140/

In addition, one must take into account that the luminescence is indirectly influenced by a series of biochemical reactions in the living bacterial cells, which are highly dependent on the metabolism of the said bacterial cells, itself putatively altered by the incoming toxicant [32,33]. Therefore, the toxic effects of the added compounds on the bacterial cells can be readily revealed via the kinetic evolution of bacterial bioluminescence, while keeping in mind their influence on the general cellular metabolism.

Although there are some reports studying the cytotoxicity of carbon-based nanomaterials [12,34], only one group of materials was studied and using wild-type bacterial cells [13,35]. In addition, toxicity experiments were conducted by using either tedious microbial plating methods [36] or using expensive bio-reagents and specialized bioanalytical kits [35]. Of special note is the fact that the bioluminescence assay described herein based on genetically modified bacterial cells is both sensitive and cost-effective, as bacterial cells produce all the needed ingredients involved in bioluminescence generation without the addition of any exogenous bio-reagents [37]. Even though engineered bacterial cells have been used to detect various toxic compounds, their application in an assay resulting from the exposure to nanomaterial toxicity has not been much exploited, with the exception found in cases of metal nanoparticles, like silver [38] or copper [39].

In this work, three different commercial carbon allotropes of 0D carbon black nanopowder (CB), 1D multiwall carbon nanotube (MWCNT) and 2D graphene nanosheet have been incubated at the same dispersal concentrations (or suspensions) with two of the aforementioned genetically engineered *E. coli* bacteria strains of DPD2794 and TV1061. The resulting bacterial bioluminescence (toxicity induction) and optical density changes (survival) are used to evaluate the cytotoxicity of carbon-based nanomaterials at two different temperatures of 30 °C and 25 °C. The field emission scanning electron microscope (FESEM) was used to observe any possible interaction or morphological effect on the bacterial cells, by the said carbon based nanomaterials. To our best knowledge, this is the first report using engineered *E. coli* bacterial bioluminescence in the toxicity study of several carbon-based nanomaterials.

2. Materials and methods

2.1. Materials

Kanamycin sulfate (K1377), LB-broth (L3032), glutaraldehyde solution (G7651), and ethanol (02877) were purchased from Sigma (Germany). Phosphate buffer saline (PBS buffer, pH 7.4) was prepared in our lab using sodium chloride (S7653), sodium phosphate dibasic (94046) and sodium phosphate monobasic (71505) received from Sigma (France). Deionized water was produced by a Millipore water purification system (Molsheim, France). Short multiwall carbon nanotubes (MWCNTs) modified with carboxylic group were purchased from Nanostructured & Amorphous Materials. Inc., graphene nanosheets were acquired from Graphene Supermarket. Inc. and carbon black nanopowders (CB, Monarch 1300) were obtained from Cabot Inc. *E. Coli* bacteria strains of DPD2794 and TV1061 were acquired from Prof. Shimshon Belkin of The Hebrew University of Jerusalem in Israel. Non-sterile white polystyrene 96 well microtiter plates (Costar, Corning Incorporated, USA) were used in the bioluminescent assays.

2.2. Medium preparation

LB (Luria-Bertani) medium was prepared by adding 2 g LB broth powder into 100 mL double distilled water in a 200 mL bottle. The bottle with the cap partially closed and covered by a piece of aluminum paper was sterilized in an autoclave-steam sterilizer (Tuttnauer, 2540 ML) for 15 min at 121 °C. After freely cooling down to room temperature, the LB medium was immediately used for the cultivation of bacteria and the preparation of various dispersed carbon-based nanomaterials dilutions.

2.3. Instrumentation

Growth of *E. coli* strain DPD2794 and TV1061 bacteria was performed using a water bath (Grant Instruments, Cambridge Ltd., UK). The optical density of bacterial suspensions was measured using a DR/ 2500 spectrophotometer Odyssey (HACH Company, USA), while various dilutions of bacterial cultures and carbon-based nanomaterials solutions were mixed using a G560E Genie2 vortex. For the centrifugation experiments, a model type Hitachi Universal 320R (Germany) was used. Bioluminescence measurements were conducted in a luminometer (Luminoskan Ascent, Thermo Fisher Scientific, United States). The morphology of carbon-based nanomaterials and bacterial cells was characterized by using the field emission electron scanning microscope (Raith e-line, Germany). We wished to evaluate the possibility that the carbonaceous materials may have been affected by the presence of the bacteria via any of their metabolites and therefore we checked for changes in their surface or structure and this by the use of infrared and Raman spectroscopy and compared against the original material.

2.4. Bacterial strains

E. coli DPD2794 and TV1061 strains were used as recombinant luminescent bioreporter bacteria. *E. coli* DPD2794 strain contains the promoter of DNA damage sensitive *recA* gene, while *E. coli* TV1061 strain harbors the promoter of heat-shock *grpE* gene; the operon of *lux*CDABE gene, used as the bioluminescent reporter, was fused with these promoters in the plasmid of two *E. coli* strains. The *grpE* gene is sensitive to metabolic changes that can be activated due to the presence of cytotoxic substances, while *recA* gene is mainly responsive to the genotoxical compounds. Before the initial growth step, the bacterial suspensions were stored at −20 °C in a sterile medium mixture containing equal volumes of LB medium and glycerol aqueous solution (40%, v/v).

2.5. Bacterial growth conditions

E. coli bacterial cultivation, prior to bioluminescence measurements, was performed in 10 mL LB medium supplemented with 10 μL of 50 mg mL^{-1} kanamycin antibiotics, with a final concentration of antibiotic at 50 μg mL^{-1}. The cells were grown for 9 h at 37 °C in a thermostated water bath. Thereafter, 200 μL of the resulting bacterial suspension were inoculated into 10 mL fresh LB medium free of antibiotics at 30 °C, to get the optical density of 0.08 as determined by a spectrophotometer, corresponding to a bacteria cell concentration number of 1.1×10^8 cfu mL^{-1}.

2.6. Preparation of the 96-well microtiter test plate

Stock solutions (0.1 mg mL^{-1} were prepared by dispersion of 1 mg of various commercial carbon-based nanomaterials in 10 mL ddH_2O, followed by ultrasonication at room temperature for 1 h. Then, 100 μL stock solution was diluted into 900 μL LB medium in a 1.5 mL Eppendorf tube to obtain a suspension of 1:10 of carbon-based nanomaterials (10 μg mL^{-1}, and thereafter tenfold serial aliquots of 10^{-2} (1 μg mL^{-1}), 10^{-3} (0.1 μg mL^{-1}), 10^{-4} (10 ng mL^{-1}), 10^{-5} (1 ng mL^{-1}) and 10^{-6} (0.1 ng mL^{-1}). To obtain uniform carbon nanomaterials/bacterial suspension, Eppendorf tubes containing mixtures of 360 μL bacterial suspension of a specific

optical density of 0.08 and 40 μL carbon-based nanomaterials (MWCNT, graphene and carbon black) solutions of different concentrations (volume ratio of bacteria:toxicant (9:1)) were prepared and vigorously shaken.

All bioluminescence measurements were performed in opaque 96-well microtiter plates containing 90 μL of the bacteria culture of different optical densities and 10 μL of a given carbon-based nanomaterial concentration. Each concentration has three replicas. The bioluminescence measurements for *E. coli* DPD2794 and TV1061 were conducted both at 30 °C and 25 °C, respectively for 5.5 h. All the experiments were repeated three times and the average value were shown in figures hereafter. Luminescence values are presented in relative light units (RLU), and the parameter of the area under curve (AUC), defined as the integration value for the bioluminescence kinetic curve over a fixed time range, was used to quantify the carbon-based nanomaterials influence onto the bacterial bioluminescence at different concentrations.

2.7. Optical density measurement of bacterial cell suspension in the presence of carbon nanomaterials

The influence of carbon nanomaterials onto the bacterial cells growth is evaluated by measuring the bacterial optical density changes in the presence of different concentrations of nanomaterial dilutions. Specifically, 100 μL of 3 different carbon nanomaterial dilutions each one containing three typical concentrations (0.1 mg mL^{-1}, 10 μg mL^{-1} and 1 ng mL^{-1}) were mixed with 900 μL of bacterial suspension and incubated for 5.5 h at 30 °C and 25 °C, respectively. Their optical density values at 600 nm were measured every 30 min using a spectrophotometer. In the control experiment, the dilutions at the same concentrations (0.1 mg mL^{-1}, 10 μg mL^{-1} and 1 ng mL^{-1}) for the three different carbon nanomaterials were prepared by using fresh LB medium and their OD changes were recorded under the same conditions without bacterial cells. All the OD measurement experiments were repeated three times and the average values were used in the following analysis.

2.8. Surface morphology characterization of carbon-based nanomaterials and engineered bacterial cells

For the characterization of surface morphology, the carbon-based nanomaterials were dispersed in ethanol (0.01 mg mL^{-1}) by ultrasonication for 30 min at room temperature, followed by deposition of one drop solution onto the clean silicon substrate, which were directly used for SEM imaging after drying.

The surface morphology of intact engineered bacterial cells and those treated with carbon-based nanomaterials were both characterized by FE-SEM. Specifically, 200 μL of bacterial or bacteria/carbon-based nanomaterials suspension was gathered from 96-well microtiter plates after the luminescence measurement. Furthermore, the resulting bacteria or bacteria/carbon nanomaterials suspension was centrifuged at 10,000 rpm for 10 min followed by two fresh PBS buffer washes. Next, the obtained bacterial cells' pellet was fixed in 500 μL glutaraldehyde aqueous solution of 2.5 wt % at 4 °C for 4 h. After fixation, the suspension was centrifuged (10,000 rpm, 5 min) and washed twice with ddH_2O, followed by a stepwise dehydration using graded ethanol aqueous solutions of 30%, 50%, 70% and 100%, respectively. Each step was conducted for 15 min at 4 °C followed by centrifugation (10,000 rpm, 5 min). Finally, the bacterial cells were dispersed in 1 mL absolute ethanol and then deposited onto a clean glass substrate, followed by sputter coating with a thin palladium layer prior to SEM imaging to suppress the charging effects.

3. Results and discussions

3.1. Description of both genetically engineered E. coli bacteria cells of three carbon-based nanomaterials

The surface morphology of engineered *E. coli* DPD2794 bacteria cells is shown in Fig. 1. After glutaraldehyde fixation and ethanol dehydration, the rod-like structure of *E. coli* DPD2794 bacterial cells is clearly observed, including actively dividing ones Fig. 1A, the single cell is measured as 1–2 μm long and around 500 nm wide. From a higher magnification image shown in Fig. 1B, the fine structures of the bacterial cell membrane and the peritrichously arranged flagella are clearly displayed. Similar surface morphology for the *E. coli* TV1061 bacteria cells is observed and the details are shown in the Supporting material (Fig. S1).

The morphology of three carbon-based nanomaterials is shown Fig. 2. The MWCNT used in this study is modified with carboxylic groups, which is responsible for their good water dispersion ability as shown in the inset of Fig. 2A. From the SEM image, the length of MWCNT is measured as 0.5–2 μm and its diameter is less than 8 nm. A water solution of graphene nanosheet is shown in the inset of Fig. 2B, where the sharp edge and the multilayer structures of graphene are clearly observed. For the carbon black nanopowder used in this study, it is also easily dispersed in water (inset of Fig. 2C). The average size of these carbon black nanopowders is around 30 nm.

The surface modification and structural properties of carbon-based nanomaterials were probed by ATR-FTIR and Raman spectroscopy and the results are shown in Fig. S2 of Supporting material. From ATR-FTIR spectra (Fig. S2A), two characteristic peaks at 1750 cm^{-1} and 1600 cm^{-1} were detected for MWCNT and carbon black, confirming their surface modification by carboxylic groups [40]. The typical Raman D, G and G′ bands at 1350 cm^{-1}, 1570 cm^{-1} and 2617 cm^{-1}, respectively, were recorded

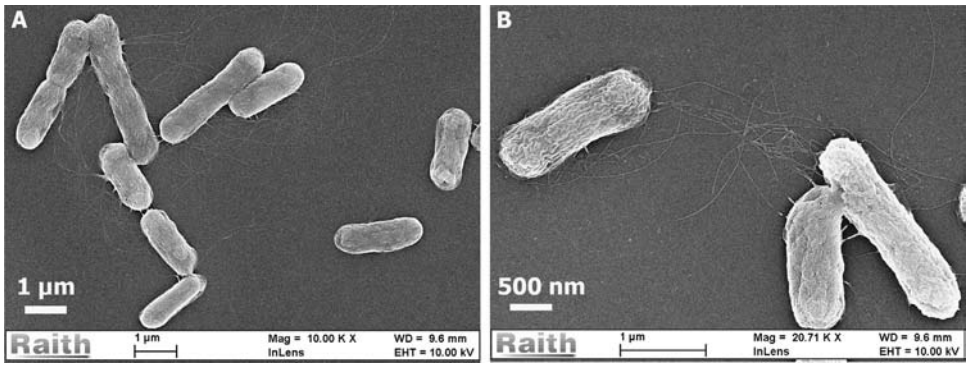

Fig. 1. The SEM images of genetically engineered *E. coli* DPD2794 bacteria cells at lower (A) and higher (B) magnifications. The bacterial cells (optical density of 0.08) are fixed with glutaraldehyde, dehydrated with ethanol solution and sputter coated with palladium prior to SEM imaging.

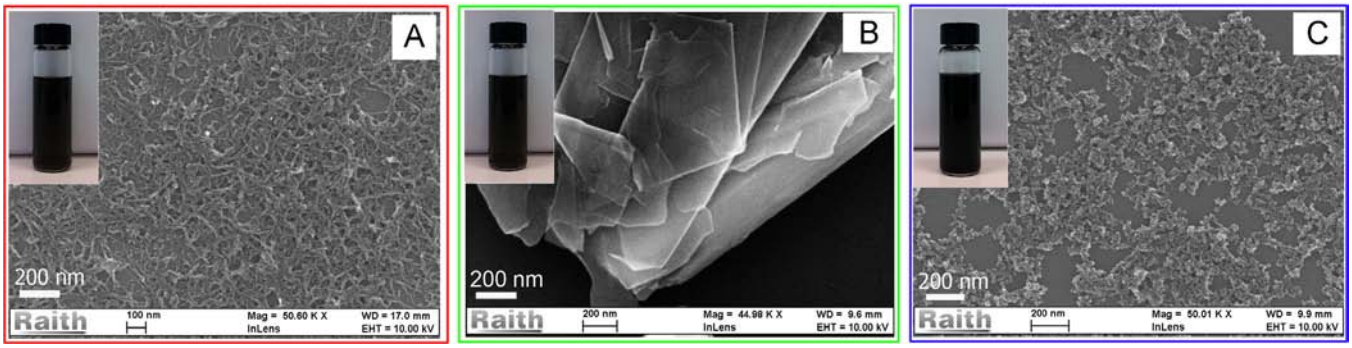

Fig. 2. SEM images of commercially available carbon-based nanomaterials: multi-wall CNTs (A), graphene nanosheet (B) and carbon black nanopowder (C). The vials containing the aqueous solution (0.1 mg mL^{-1}) of different carbon-based nanomaterials are shown in the inset of the corresponding SEM images. The three different carbon-based nanomaterials were dispersed in ethanol (0.01 mg mL^{-1}) via ultrasonication and deposited onto clean silicon substrates for SEM imaging.

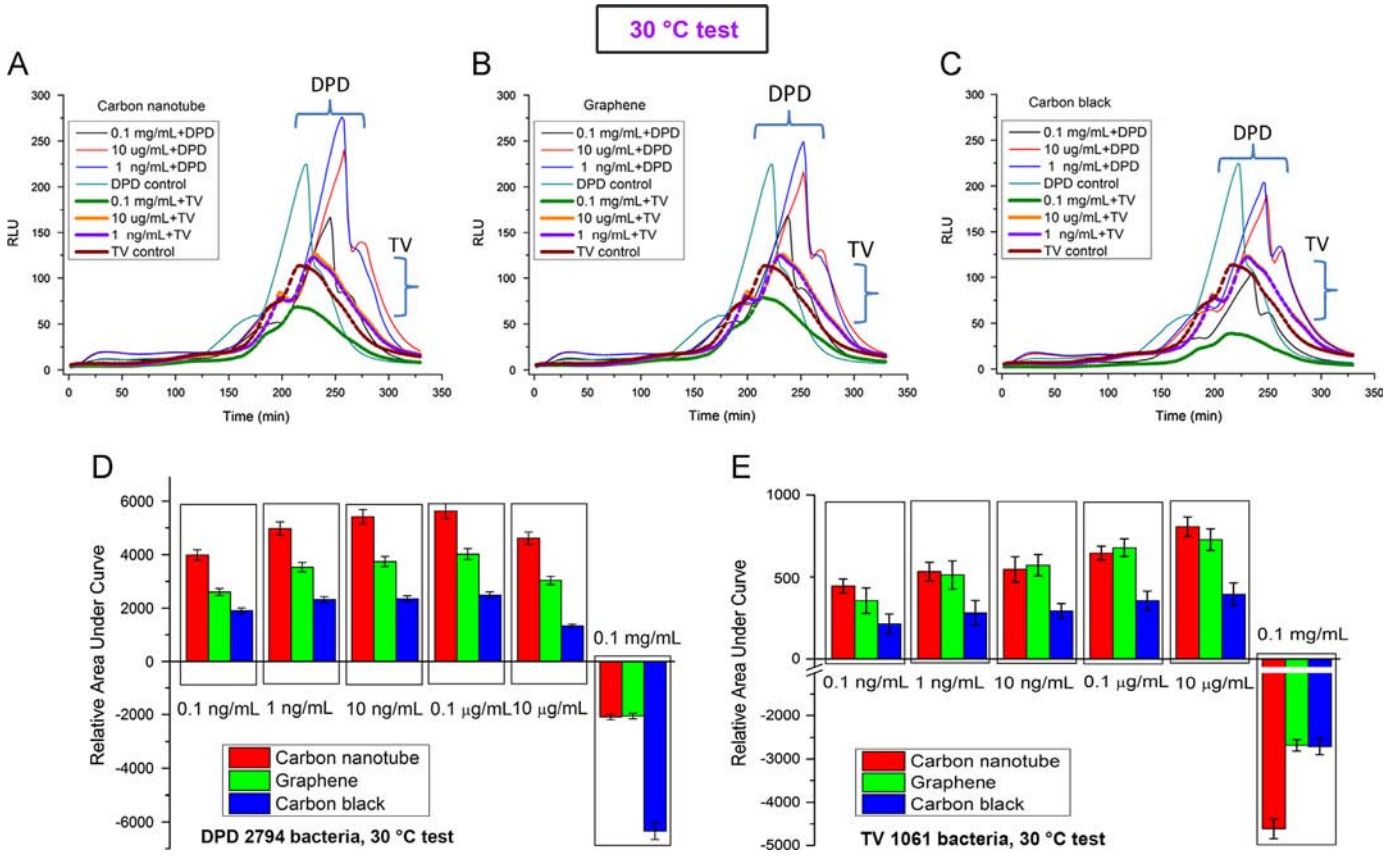

Fig. 3. The bioluminescence of bacterial strains of *E. coli* DPD2794 and *E. coli* TV1061 in the presence of MWCNT (A), graphene nanosheet (B) and carbon black nanopowder (C) and the bioluminescent relative area under the curve versus different concentrations of carbon-based nanomaterials for *E. coli* DPD2794 (D) and *E. coli* TV1061 (E). The bacterial bioluminescence is recorded at 30 °C.

for the three carbon-based nanomaterials with different relative intensities, and more details are explained in the Supporting material (Fig. S2B).

3.2. Bacterial bioluminescence induced by carbon-based nanomaterials

Bacterial bioluminescence induced by three carbon-based nanomaterials has been recorded at 30 °C with two *E. coli* strains DPD2794 and TV1061 (Fig. 3), which was found to be an optimized temperature for the bioluminescent assay [41]. Different concentrations from all the three carbon-based nanomaterials can be differentiated based on their maximum bioluminescent peak for *E. coli* DPD2794, while in the particular case of *E. coli* TV1061 bacteria only high and low toxicity of carbon nanomaterials were differentiated. Specifically, in the presence of both MWCNT and graphene, bacterial bioluminescence of *E. coli* DPD2794 was induced in a much stronger manner than that of the control concentrations at lower than the stock solution 0.1 mg mL^{-1} (Fig. 3A and B). Interestingly, in the case of carbon black, bacterial bioluminescence is inhibited at all the concentrations tested (Fig. 3C), possibly due to it's higher toxicity. All three carbonaceous nanomaterials similarly affect *E. coli* TV1061 bacterial bioluminescence response: the highest tested content of 0.1 mg mL^{-1} inhibited overall bacterial bioluminescence, while two lower diluted contents of 10 μg mL^{-1} and 1 ng mL^{-1} were both shown to induce bioluminescence. Since several peaks appear over time, thus, the area under the curve (AUC) value was the preferred parameter (Fig. 3A–C) to comparatively evaluate the induction

potential of three carbon-based nanomaterials tested. The relative area under the curve, which is obtained by subtracting that of the bacterial control, is displayed for each concentration of carbon-based nanomaterials for both *E. coli* DPD2794 (Fig. 3D) and TV1061 (Fig. 3E) strains. All three carbonaceous nanomaterials exhibit similar behaviors with *E. coli* DPD2794, where bacterial bioluminescence is induced by the presence of lower concentrations (less than 10 $\mu g\,mL^{-1}$), while the highest tested concentration of 0.1 $mg\,mL^{-1}$, resulted in a decrease of bacterial bioluminescence, with the carbon black nanopowder showing the highest cytotoxicity. Unfortunately, no proper correlations were obtained with the *E. coli* TV1061 strain thus, confirming the fact that not all bioreporters may be useful in such a test.

We repeated the same tests at an alternative temperature of 25 °C, with both *E. coli* strains DPD2794 and TV1601, but both seemed to exhibit bioluminescence responses to varying concentration of carbon-based nanomaterials which did not provide reliable dichotomous information enabling to correlate easily between materials and their concentrations versus induction. These results are shown in the Supporting material (Fig. S3).

In order to evaluate whether bacterial growth occurs during bioluminescence measurements, its OD value evolution over 5.5 h was recorded for both *E. coli* strains at both tested temperatures (25 °C and 30 °C). A typical OD temporal evaluation for MWCNT-stressed *E. coli* DPD2974 at 30 °C is shown as an example in Fig. S4, which also includes control OD data using MWCNT dilutions in the LB medium in the absence of bacterial cells as well as bacterial cells alone free of carbonaceous materials. The graph clearly states that the OD evolution pattern is mostly unaffected by the lower suspensions of carbonaceous materials and the growth itself seems a little slowed (indication of possible inhibition) but manages to evolve in a similar way, implying that we do not really need to take into consideration growth evolution. There is however no correlation between the AUC and the various carbon nanomaterial concentrations.

3.3. Morphology of carbon-based nanomaterials treated with bacterial cells

In order to elucidate any putative interaction between bacterial cells and the three different carbonaceous nanomaterials, their

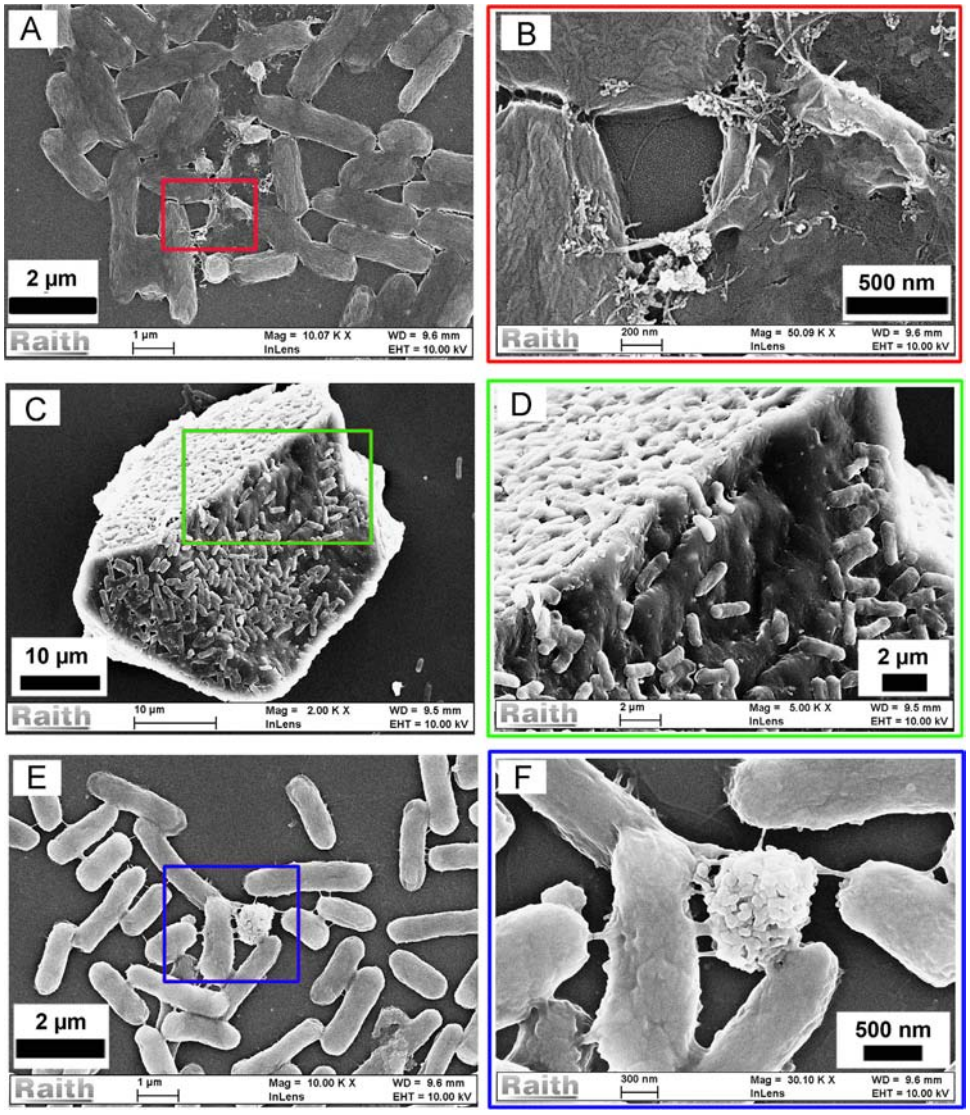

Fig. 4. SEM images of *E. coli* DPD2794 bacterial cells treated with MWCNT (A, B), graphene nanosheet (C, D) and carbon black nanopowder (E, F). For each figure in the left column, a rectangle marked area is magnified and the details are shown in the right column. These carbon-based nanomaterials/bacterial suspensions were already subject to the bioluminescence measurement at 30 °C for 5.5 h prior to their SEM imaging.

combined resulting morphology, once the bioluminescence measurement was carried out, was observed via SEM imaging as shown in Fig. 4. COOH-functionalized MWCNT (Fig. 4A,) were clearly aggregated at the end of the bacterial cells and these were likely bundled with their flagella or pili (Fig. 4B). According to a published report [36], the direct piercing effects into bacterial cells was responsible for their cytotoxicity, however, it was not here observed possibly due to a different surface modification of the MWCNTs. The graphene-based nanosheets were covered by the bacterial cells (Fig. 4C), in a fairly homogeneous way in a firm manner (Fig. 4D). It should be noted that others have shown that treated forms of graphene may prevent biofilm formation [42] and the extremely sharp edge of graphene nanosheet may pierce into the bacteria [15,16]. In the case of carbon black nanopowder, it was found that there are some bridges formed whose diameter are larger than that of pili and are worthy of an additional study in themselves (Fig. 4E and F).

4. Conclusions

In this report, two engineered *E. coli* bacterial bioreporter strains DPD2794 and TV1061 were used to evaluate the cytotoxicity of three carbonaceous nanomaterials, MWCNT, graphene nanosheets and carbon black nanopowder. The DNA damage sensitive *E. coli* DPD2794 strain was capable of distinguishing the various concentrations of all three carbon-based nanomaterials at 30 °C, while the heat-shock sensitive *E. coli* TV1061 bacterial cells were only able to provide partial discrimination regardless of the test temperature. The carbon black nanopowder showed the highest cytotoxicity towards the bacterial bioreporter cells out of three tested carbon-based nanomaterials, which could be due to their smaller size and better aqueous dispersion. SEM was used to characterize the morphological interaction of bacterial cells treated with all three carbon-based nanomaterials. We show herein that engineered bacterial bioreporter cells can provide indication of cytotoxicity of nanomaterials in a dose-response manner, and that these are both quick and cheap to run, enabling high throughput.

Acknowledgments

The authors are grateful to the French Ministry of Foreign Affairs and the Israeli Ministry of Science for funding their project 'Nanochip platform for water probing pollutants' under Research Networks Programs 2009–2011. The authors also appreciate the financial support from the Stratégique Program 2009–2012 of the University of Technology of Troyes (UTT) and the NANO'MAT project from the Champagne-Ardenne Region of France. Mr. Xavier Gassman of the UTT is thanked for his sustained scientific collaborative support. Prof. Robert S. Marks thanks the Singapore National Research Foundation CREATE program 'Nanomaterials for Energy and Water Management' for its financial support. K. Jia kindly thanks the Chinese Scholarship Council (CSC) (Grant number [2010]6030) for funding his PhD fellowship in France from September 2010 to February 2014.

Appendix A. Supporting information

Supplementary data associated with this article can be found in the online version at http://dx.doi.org/10.1016/j.talanta.2014.03.024.

References

[1] J.L. Chen, X.P. Yan, K. Meng, S.F. Wang, Anal. Chem. 83 (2011) 8787–8793.
[2] C.B. Jacobs, M.J. Peairs, B.J. Venton, Anal. Chim. Acta 662 (2010) 105–127.
[3] Y. Shao, J. Wang, H. Wu, J. Liu, I.A. Aksay, Y. Lin, Electroanalysis 22 (2010) 1027–1036.
[4] M. Pumera, Energy Environ. Sci. 4 (2011) 668–674.
[5] W.H. Shin, H.M. Jeong, B.G. Kim, J.K. Kang, J.W. Choi, Nano Lett. 12 (2012) 2283–2288.
[6] H.Y. Mao, S. Laurent, W. Chen, O. Akhavan, M. Imani, A.A. Ashkarran, M. Mahmoudi, Chem. Rev. 113 (2013) 3407–3424.
[7] Z.M. Markovic, L.M. Harhaji-Trajkovic, B.M. Todorovic-Markovic, D.P. Kepić, K.M. Arsikin, S.P. Jovanović, A.C. Pantovic, M.D. Dramićanin, V.S. Trajkovic, Biomaterials 32 (2011) 1121–1129.
[8] Z. Spitalsky, D. Tasis, K. Papagelis, C. Galiotis, Prog. Polym. Sci. 35 (2010) 357–401.
[9] Y. Zhan, X. Yang, H. Guo, J. Yang, F. Meng, X. Liu, J. Mater. Chem. 22 (2012) 5602–5608.
[10] S. Kang, M.S. Mauter, M. Elimelech, Environ. Sci. Technol. 43 (2009) 2648–2653.
[11] S. Liu, L. Wei, L. Hao, N. Fang, M.W. Chang, R. Xu, Y. Yang, Y. Chen, ACS Nano 3 (2009) 3891–3902.
[12] S. Kang, M. Herzberg, D.F. Rodrigues, M. Elimelech, Langmuir 24 (2008) 6409–6413.
[13] S. Liu, A.K. Ng, R. Xu, J. Wei, C.M. Tan, Y. Yang, Y. Chen, Nanoscale 2 (2010) 2744–2750.
[14] C.D. Vecitis, K.R. Zodrow, S. Kang, M. Elimelech, ACS Nano 4 (2010) 5471–5479.
[15] O. Akhavan, E. Ghaderi, ACS Nano 4 (2010) 5731–5736.
[16] S. Liu, T.H. Zeng, M. Hofmann, E. Burcombe, J. Wei, R. Jiang, J. Kong, Y. Chen, ACS Nano 5 (2011) 6971–6980.
[17] K. Krishnamoorthy, M. Veerapandian, L.-H. Zhang, K. Yun, S.J. Kim, J. Phys. Chem. C 116 (2012) 17280–17287.
[18] J. Tang, Q. Chen, L. Xu, S. Zhang, L. Feng, L. Cheng, H. Xu, Z. Liu, R. Peng, ACS Appl. Mater. Interfaces 5 (2013) 3867–3874.
[19] W. Hu, C. Peng, W. Luo, M. Lv, X. Li, D. Li, Q. Huang, C. Fan, ACS Nano 4 (2010) 4317–4323.
[20] T. Sreeprasad, M.S. Maliyekkal, K. Deepti, K. Chaudhari, P.L. Xavier, T. Pradeep, ACS Appl. Mater. Interfaces 3 (2011) 2643–2654.
[21] K. Hakkila, T. Green, P. Leskinen, A. Ivask, R. Marks, M. Virta, J. Appl. Toxicol. 24 (2004) 333–342.
[22] K. Jia, E. Eltzov, T. Toury, R.S. Marks, R.E. Ionescu, Ecotoxicol. Environ. Saf. 84 (2012) 221–226.
[23] R. Pedahzur, B. Polyak, R. Marks, S. Belkin, J. Appl. Toxicol. 24 (2004) 343–348.
[24] A. Ivask, T. Green, B. Polyak, A. Mor, A. Kahru, M. Virta, R. Marks, Biosens. Bioelectron. 22 (2007) 1396–1402.
[25] S. Jouanneau, M.-J. Durand, P. Courcoux, T. Blusseau, G. Thouand, Environ. Sci. Technol. 45 (2011) 2925–2931.
[26] B. Polyak, E. Bassis, A. Novodvorets, S. Belkin, R. Marks, Water Sci. Technol. 42 (2000) 305–311.
[27] B. Polyak, E. Bassis, A. Novodvorets, S. Belkin, R.S. Marks, Sensor. Actuat. B 74 (2001) 18–26.
[28] Y. Rozen, A. Nejidatl, K.-H. Gartemann, S. Belkin, Chemosphere 38 (1999) 633–641.
[29] S. Girotti, E.N. Ferri, M.G. Fumo, E. Maiolini, Anal. Chim. Acta 608 (2008) 2–29.
[30] T.K. Van Dyk, W.R. Majarian, K.B. Konstantinov, R.M. Young, P.S. Dhurjati, R.A. Larossa, Appl. Environ. Microbiol. 60 (1994) 1414–1420.
[31] A.C. Vollmer, S. Belkin, D.R. Smulski, T.K. Van Dyk, R.A. LaRossa, Appl. Environ. Microbiol. 63 (1997) 2566–2571.
[32] J. Engebrecht, K. Nealson, M. Silverman, Cell 32 (1983) 773–781.
[33] E.A. Meighen, Microbiol. Rev. 55 (1991) 123–142.
[34] L.R. Arias, L. Yang, Langmuir 25 (2009) 3003–3012.
[35] S. Kang, M.S. Mauter, M. Elimelech, Environ. Sci. Technol. 42 (2008) 7528–7534.
[36] Y.F. Young, H.J. Lee, Y.S. Shen, S.H. Tseng, C.Y. Lee, N.H. Tai, H.Y. Chang, Mater. Chem. Phys. 134 (2012) 279–286.
[37] H. Harms, M.C. Wells, J.R. van der Meer, Appl. Microbiol. Biotechnol. 70 (2006) 273–280.
[38] E.T. Hwang, J.H. Lee, Y.J. Chae, Y.S. Kim, B.C. Kim, B.I. Sang, M.B. Gu, Small 4 (2008) 746–750.
[39] F. Li, C. Lei, Q. Shen, L. Li, M. Wang, M. Guo, Y. Huang, Z. Nie, S. Yao, Nanoscale 5 (2013) 653–662.
[40] L. Vaisman, G. Marom, H.D. Wagner, Adv. Funct. Mater. 16 (2006) 357–363.
[41] K. Jia, E. Eltzov, R.S. Marks, R.E. Ionescu, Ecotoxicol. Environ. Saf. 96 (2013) 61–66.
[42] S. Yin., Y. Goldovsky, M. Herzberg, L. Liu, H. Sun, Y. Zhang, X. Cao, D.D. Sun, H. Chen, A. Kushmaro, X. Chen, Adv. Funct. Mater. 23 (2013) 2972–2978.